Enhancement of fracture strain during abrupt orthogonal strain-path changes in ferrite/martensite dual phase steel

MATSUNO Takashi[1,a *], KINOSHITA Nanami[1,b], HOKIMOTO Keisuke[1,c], HAMA Takayuki[2,d] and HONDA Yoshiaki[3,e]

[1]Faculty of Engineering, Tottori University, 4-101 Koyama-cho-minami, Tottori, Tottori 680-8552, Japan

[2]Graduate School of Energy Science, Kyoto University, Yoshida-Honmachi, Sakyo-ku, Kyoto 606-8501, Japan

[3]Nippon Steel Corporation, 20-1 Shintomi, Futtsu-City, Chiba, 293-8511 Japan

[a]matsu@tottori-u.ac.jp, [b]m23J3015z@edu.tottori-u.ac.jp, [c]b20T1092z@edu.tottori-u.ac.jp, [d]hama@energy.kyoto-u.ac.jp, [e]honda.x66.yoshiaki@jp.nipponsteel.com

Keywords: Ductile Fracture, Strain-Path Change, Post-Necking, Dual Phase Steel

Abstract In multistage press forming, the scrutiny of work-hardening behavior attributed to abrupt strain path changes in deformation paths has been pivotal in the context of press formability. However, applying this method to stretch flanging presents a formidable complexity. In such scenarios, substantial deformations resulting from shear-cut processing and subsequent stretch-flange formation significantly influence the local fracture strains, a critical determinant of process success. Therefore, our investigation examined the impact of deformation path variations on the fracture strain of dual-phase steel sheets. A crucial facet of our experimental approach involved manipulating the strain level during the initial tensile deformation. Tensile deformation was extended beyond the onset of necking, culminating in the emergence of microvoids within the material. Following this preliminary extensive strain, successive tensile tests were conducted on diminutive round-bar specimens, subject to a 90º change in the deformation path, to investigate their influence on work hardening and fracture strain. The outcomes of the diameter-measuring tensile tests unveiled a pronounced cross effect during the early stages of deformation, particularly concerning work-hardening behavior. However, as the deformation advanced, the results conformed to the stress-strain curve observed in the same direction of tension. Notably, the fracture strain exhibited an approximately 10% enhancement attributable to the abrupt strain path change, thereby having the potential to augment the practical stretch flangeability.

Introduction

In press forming, the deformation path of a material commonly changes partway through the process. Processes involving multiple dies, such as progressive presses, often entail abrupt alterations in the deformation paths. Forming processes like stretch flanging may incorporate a 90º abrupt strain path change, particularly when the initial deformation is characterized as shear-cut processing. The ductility of automotive crash-resistant components, which are manufactured via press forming, depends on how they respond to an abrupt strain path change between press forming and crushing deformations.

Dortance, feespite its impw reports address the fracture strain associated with sudden changes in the deformation path (local plastic strain at fracture). In single-phase steels, an abrupt strain path change only alters work hardening, with minimal impact on elongation [1]. However, elongation increases due to an abrupt strain path change in multi-phase steels like ferrite-pearlite steels [1].

Therefore, this study investigates work hardening and fracture strain in response to pre-strain surpassing plastic instability in dual-phase (DP) steels. Tiny round bar tensile specimens were cut

from sheet-type tensile tested specimens that had undergone pre-straining exceeding the onset of necking. Subsequent diameter measurement-type tensile tests were executed [2-4] in the same direction and at a 90° angle to the pre-strain.

Experimental Methods

Material

Two DP steels, DP-A and DP-B, with tensile strengths of 560 and 650 MPa, respectively, were used for the tests. The chemical compositions and mechanical properties are detailed in **Tables 1** and **2**, respectively. These materials exhibited hard martensite islands dispersed within a soft ferrite matrix. **Figure 1** shows the micrographs of these microstructures. Specifically, DP-A and DP-B comprised 4.3% and 10.5% martensite volume fraction, respectively.

Table 1 Chemical components of tested steels (mass%)

	C	Si	Mn
DP-A	0.038	0.50	1.50
DP-B	0.067	0.50	1.50

Table 2 Mechanical properties of tested steels

	Yield stress [MPa]	Tensile strength [MPa]	Uniform elongation [%]	Total elongation [%]
DP-A	335	561	19	31
DP-B	353	650	16	24

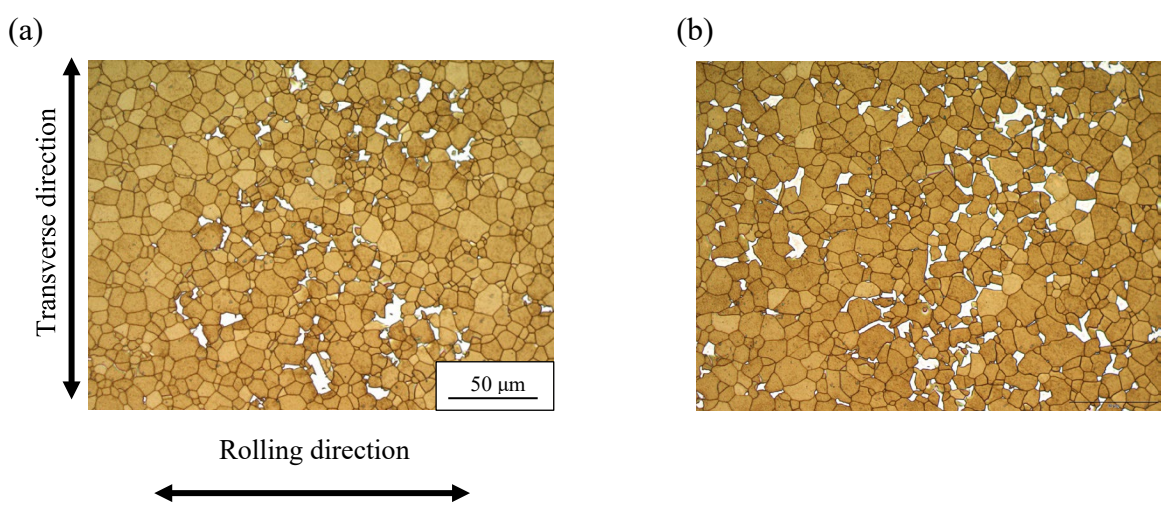

Fig. 1 Micrographs of the DP steels used in this study: (a) DP-A containing 4.3% martensite and (b) DP-B containing 10.5% martensite. Grains colored in white are martensite, and remaining brown grains are ferrite.

Preparing tiny round-bar specimen

We subjected No. 5 type specimens, 2.5-mm thick and standardized by Japanese Industrial Standards (JIS) Z2241, to preliminary tensile testing before subsequent compact tensile tests. These specimens were elongated by up to 23.14% and 19.44% for DP-A and DP-B, respectively,

surpassing their uniform elongations of 19% and 16%, as indicated in **Table 2**. Prior to the compact tensile tests, which involved real-time diameter measurements, the specimens experienced necking due to deformations exceeding their uniform elongation.

As depicted in **Fig. 2**, the preliminary tensile test was aligned such that the tensile direction of the tiny round-bar specimens corresponded to the transverse direction of the cold-rolling process (referred to as the transverse direction). Accordingly, the JIS No. 5 specimens were tensioned in the transverse direction without a strain path change (**Fig. 2a**) and in the rolling direction in the presence of an orthogonal strain path change (**Fig. 2b**).

The design of the tiny round-bar specimens is presented in **Fig. 3**. The thinnest part of these specimens had a diameter of 1.0 mm, enabling their extraction from the JIS No. 5 specimens that had undergone pre-straining exceeding the onset of necking.

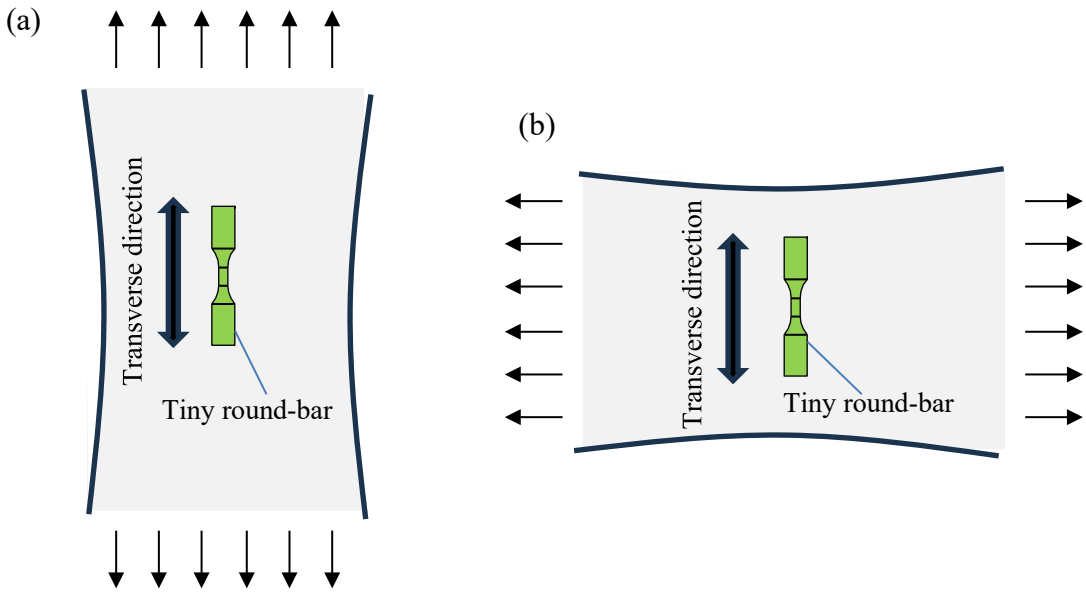

Fig. 2 Sampling position of the tiny round-bar specimens and the tensile direction of the JIS No. 5 tensile test prior to compact tensile testing: (a) without subsequent strain path change and (b) with a subsequent orthogonal strain path change.

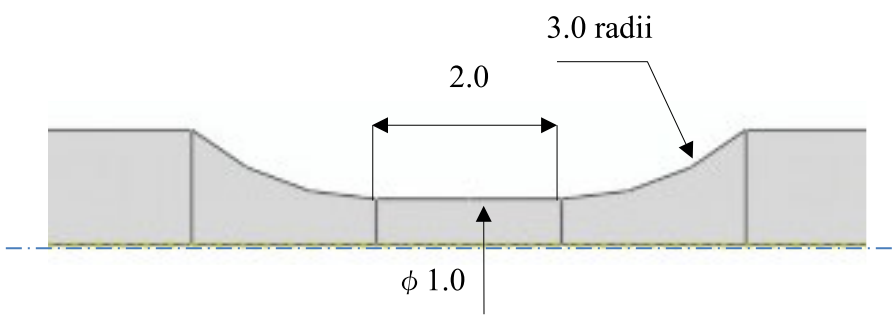

Fig. 3 Geometry of the tiny round-bar specimen depicted in an axisymmetric two-dimensional drawing.

Compact tensile test with real-time diameter measurements

After extracting the tiny round-bar specimens, compact tensile tests with real-time diameter measurements were executed, generating true stress versus cross-sectional reduction area (CSRA,

ρ) curves. In these compact tensile tests, the diameters, D_a and D_b, of the thinnest cross-sectional area under tension were continuously measured in two directions. The specimen was oriented such that D_b corresponded to the thickness of the original steel material. The true stress σ_t and ρ in the cross-section were calculated as follows:

$$\sigma_t = \frac{4F}{\pi D_a D_b}, \tag{1}$$

$$\rho = \ln\left(\frac{D_{0^2}}{D_a D_b}\right), \tag{2}$$

where D_0 corresponds to the initial diameter of the specimen (1.0 mm).

Results and discussion

Figure 4 illustrates the σ_t $-\rho$ curves measured for DP-A and DP-B. In the materials subjected to orthogonal abrupt strain path changes (referred to as the "orthogonal-loading case"), an increased initial yield stress was observed compared to those deformed in the same direction as the pre-strain (referred to as the "same-direction case"), although their subsequent σ_t decreased. Notably, the same-direction and orthogonal-loading cases reached peak loads at $\rho = 0.01$ and $\rho = 0.03$, respectively, marking the onset of necking in the specimens.

In DP-A (**Fig. 4a**), at the marked final point on the plot, the cross-sectional reduction area (CSRA) ρ was 0.92 for the orthogonal-loading case, compared to $\rho = 0.87$ for the same-direction case, indicating a marginal enhancement in the fracture strain. Given the challenges in precisely determining the fracture timing in the σ_t $-\rho$ curves, the definitive ρ was deduced from scanning electron microscope (SEM) images of the fracture surface (**Fig. 5**). The fracture surface areas were quantified from these images. As a result, a comparative analysis between the same direction (**Fig. 5a**) and orthogonal-loading cases (**Fig. 5b**) also exhibited a 0.09 increase in ρ. Previous studies have suggested that in multi-phase steels, an abrupt strain path change can relocate sites of microscopic plastic deformation, which is considered to alleviate deformation localization during pre-straining and thereby augment ductility. This study hypothesized a similar phenomenon in the DP steels, albeit with a relatively minor effect. Variations in work hardening and resultant stress states may obscure microscopic enhancement in ductility.

In the case of DP-B, the impact of a strain path change on the σ_t $-\rho$ curves was less significant than DP-A (**Fig. 4b**). The improvement stemming from the strain-path change was modest but contributed to increased fracture strain. Final ρ values on the σ_t $-\rho$ curve were 0.55 and 0.58 for the same-direction and orthogonal-loading cases, respectively. SEM images of the fracture surfaces (**Figs. 5c** and **5d**) unveiled a 0.1 increase in the actual final ρ, mirroring the observation in DP-A. It suggests that the martensite volume fraction does not markedly influence the effect of strain path change on the increase in fracture strain.

An additional consideration pertains to the disparity in anisotropy. **Fig. 6** illustrates the history of D_b/D_a relative to ρ. Lower values signify a flattened elliptical shape in the thickness direction. The behaviors observed in DP-A(**Fig. 6a**) and DP-B(**Fig. 6b**) are akin. Therefore, we focus on DP-A to discuss its anisotropy: For ρ lower than approximately 0.45, D_b/D_a was marginally smaller for the same-direction cases than for the orthogonal-loading cases. The relationship started to invert, commencing from approximately $\rho = 0.45$ with an intensified flattening in the thickness direction in the abrupt strain path change of materials. In orthogonal-loading cases, no flattening occurred until ρ reached approximately 0.08, after which D_b/D_a decreased sharply. This flattening of the cross-section indicates more pronounced necking in the section involving D_b, potentially leading to a transformation into a geometry with higher triaxiality, which might diminish the impact on the enhanced fracture strain.

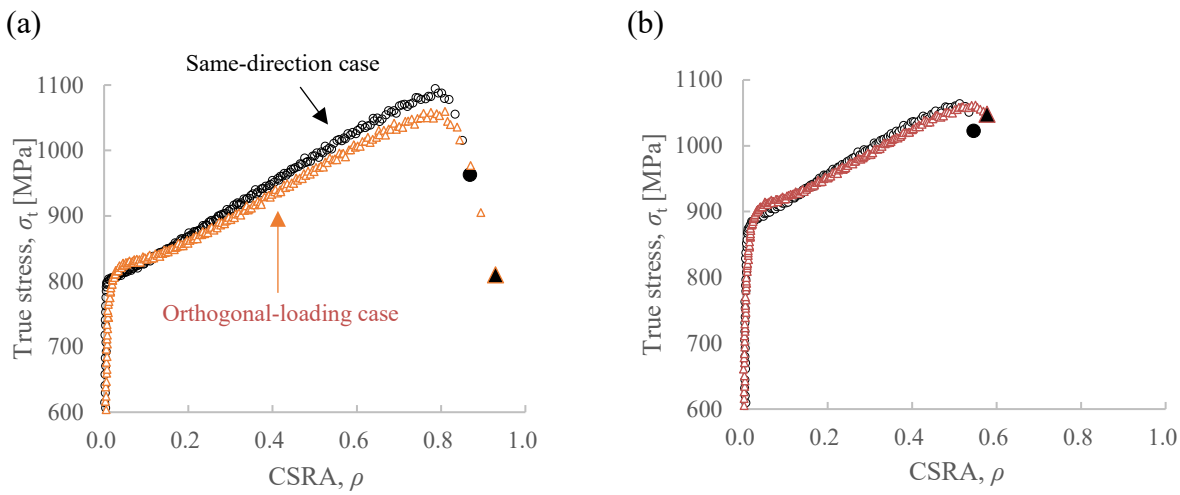

Fig. 4 True stress σ_t versus cross-sectional reduction area (CSRA) ρ: (a) DP-A and (b) DP-B.

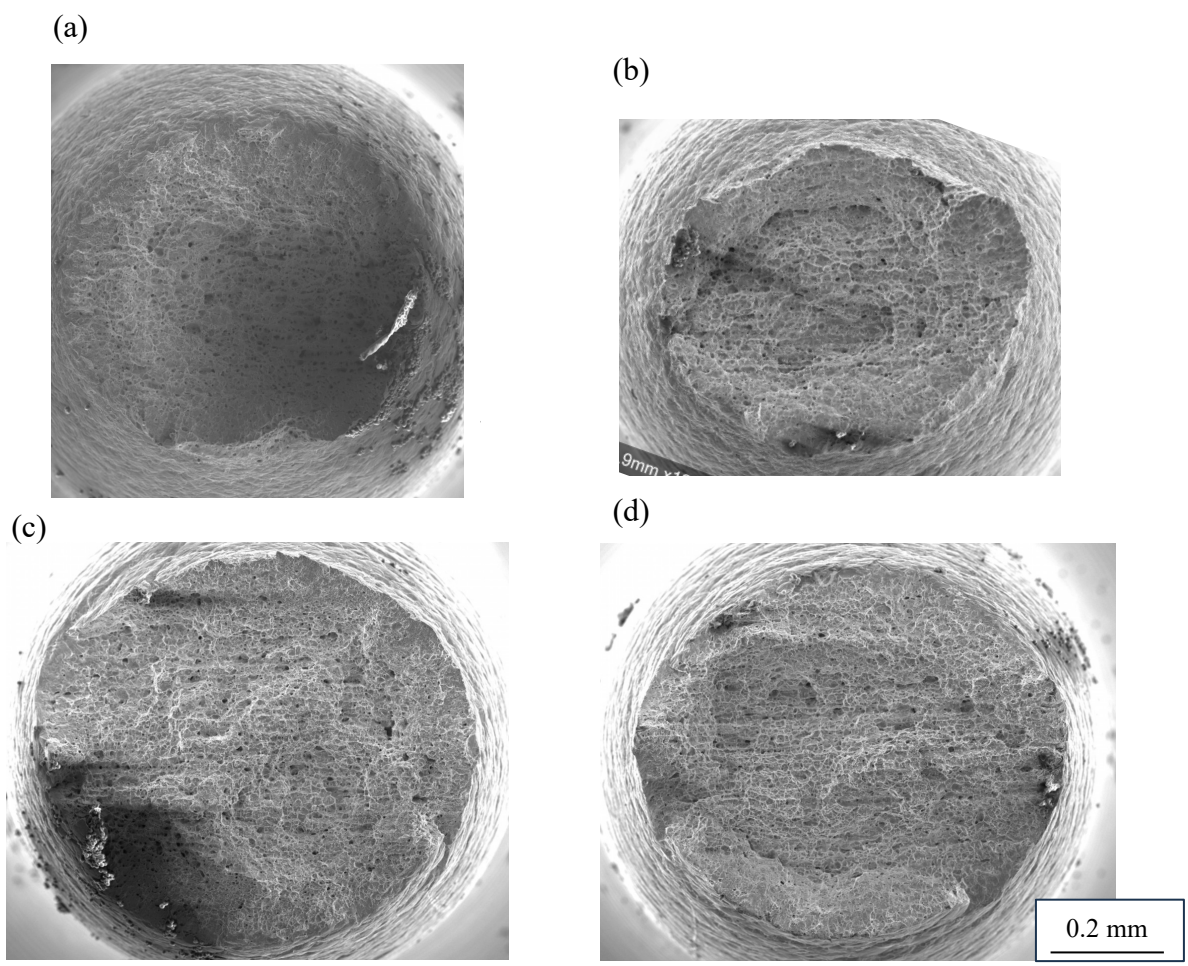

Fig. 5 SEM images of fracture surface: (a) same-direction case for DP-A ($\rho = 0.95$), (b) orthogonal-loading case for DP-A ($\rho = 1.04$), (c) same-direction case for DP-B ($\rho = 0.60$), and (d) orthogonal-loading case for DP-B($\rho = 0.70$).

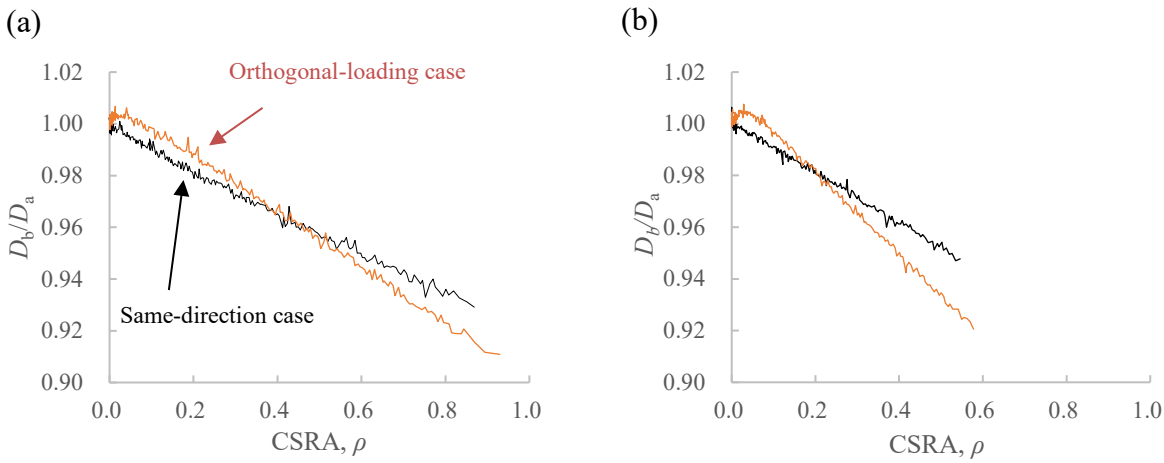

Fig. 6 D_b/D_a versus CSRA ρ: (a) DP-A and (b) DP-B.

Summary

This study investigated the impact of enhancing fracture strain during an abrupt orthogonal strain path change in two types of DP steels with different martensite volume fractions. The results validated an improvement in fracture strains for both types of DP steels, with enhancements of 0.1. While this quantitative behavior differs from that observed in ferrite-pearlite steels, it may significantly contribute to press-formability in processes like stretch-flange forming, where a difference of 0.1 in fracture strain holds substantial importance. We postulated that the degree of improvement in fracture strain due to the abrupt strain path change was influenced not only by the previously reported microscopic deformation concentration mechanisms but also by variations in anisotropy and work-hardening behavior.

References

[1] T. Yasutomi, T. Matsuno, E. Sakurada, S. Yonemura, H. Shoji, M. Ohata, Ductile Fracture Behavior for Two-phase Steel under Tensile Deformation with Strain Path Change, Tetsu-to-Hagane, 108(2022) 772-783(In Japanese). https://doi.org/10.2355/tetsutohagane.TETSU-2022-020

[2] T. Matsuno, D. Kondo, T. Hama, T. Naito, Y. Okitsu, S. Hayashi, K. Takada, Flow stress curves for 980MPa- and 1.5GPa-class ultra-high-strength steel sheets weakened under high-stress triaxiality, Int. J. Mech. Sci., 261(2024), 108671. https://doi.org/10.1016/j.ijmecsci.2023.108671

[3] T. Matsuno, T. Fujita, T. Matsuda, T. Shibayama, T. Hojo, I. Watanabe, Unstable stress-triaxiality development and contrasting weakening in two types of high-strength transformation-induced plasticity (TRIP) steels: Insights from a new compact tensile testing method, J. Mater. Process. Technol., 322(2023), 118174. https://doi.org/10.1016/j.jmatprotec.2023.118174

[4] T. Matsuno, T. Hojo, I. Watanabe, A. Shiro, T. Shobu, K. Kajiwara, Tensile deformation behavior of TRIP-aided bainitic ferrite steel in the post-necking strain region, Sci. Tech. Adv. Mater.: Methods, 1(2021), 56-74. https://doi.org/10.1080/27660400.2021.1922207